

Electro-Optic Frequency Offset Estimator for Optical OFDM

Jokhakar Jignesh⁽¹⁾, Bill Corcoran^(1,2), Chen Zhu⁽¹⁾, Arthur Lowery^(1,2)

⁽¹⁾ Electro-Photonics Lab, Dept. of Elec. and Comp. Sys. Monash Univ. jignesh.jokhakar@monash.edu

⁽²⁾ Centre of Ultrahigh-bandwidth Devices for Optical Systems (CUDOS), Australia.

Abstract We present a new design for an electro-optic carrier frequency offset (CFO) estimator for optical OFDM systems, and experimentally demonstrate CFO estimation using off-the-shelf components, capable of tracking up to ± 500 MHz offsets from a 28-Gbaud OFDM signal.

Introduction

Coherent optical communication supports expanded capacity and longer distance transmission by enabling complex modulation and higher receiver sensitivity. Optical OFDM is considered a strong candidate for upcoming 400G and 1 Tbps super-channel systems. In coherent receivers, offsets between the local oscillator and incoming signal necessitates carrier recovery. Among these steps is frequency offset estimation, which is particularly critical in OFDM systems to properly align the Fourier transform with the subcarriers to prevent loss of orthogonality.

In present systems, carrier recovery is performed by digital signal processing (DSP); for example, the CFO can be estimated by finding the maximum of the absolute of the FFT of the signal samples [1]. However, high-speed DSP can lead to significant latency and high power consumption in transceivers. To overcome these issues, alternate CFO estimation methods have been proposed, including optical injection locking (IL) [2], optical phase locked loops (OPLL) [3] and electro-optic phase-locked loops (EOPLL) [4]. Although these techniques have their own advantages, such as phase noise mitigation along with CFO estimation and possible sequential architecture, they are restricted by sub-system complexity and/or the bandwidths of the components required.

We propose a novel design that estimates the CFO of an optical OFDM system by electro-optic processing. Our technique uses a relatively simple topology, which performs over a wider range of frequency offsets for high baud rate signals compared with the approaches above. Our device has the potential for real-time CFO estimation, reduces the DSP processing load, and uses off-the-shelf components.

Theory and design

The concept of the FO estimator is based on the cyclostationary property of OFDM signals with cyclic prefixes, where the autocorrelation of the OFDM signal with a specific delay can give an estimate of the frequency offset [5]. This can be

achieved electro-optically as shown in Fig 1.

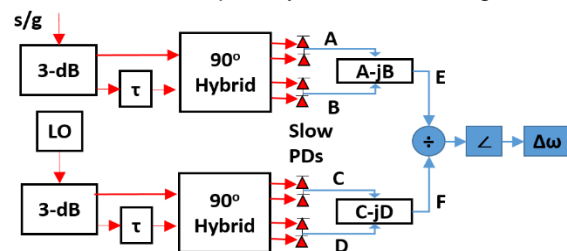


Fig. 1: CFO estimator design; PC: polarization controller, PBS: polarization beam splitter, PD: photodiode

The autocorrelation (AC) can be measured using self-coherent receivers with delays in the local-oscillator (LO) arm [6], which gives the product $z(t) \times z^*(t+\tau)$ for any input $z(t)$. The slow photodiodes (PDs) at the hybrid outputs effectively integrate this product, generating the AC [7]. This process can further be enhanced with an electrical low-pass filter at the output.

In Fig. 1, autocorrelations of both the incoming and the LO are performed. The angle of the division of these autocorrelations gives the frequency offset. Consider the received signal $E_s(t) = A_s(t)e^{j\omega_0 t}$ and LO signal $E_L(t) = A_L(t)e^{j(\omega_L t + \phi)}$ where ω_0 is the set carrier frequency, $\omega_L = \omega_0 + \Delta\omega$ is the LO frequency with $\Delta\omega$ the frequency offset between signal and LO, ϕ is the offset phase and $A_s(t)$ and $A_L(t)$ the complex field envelopes of the local oscillator and signal respectively. The optical fields E and F (see Fig. 1) are:

$$\begin{aligned} E &= \int E_s(t) \times E_s^*(t + \tau) \\ &= \int A_s(t) \times A_s^*(t + \tau) e^{-j\omega_0 t} \cdot e^{-j\omega_0 (t + \tau)} \end{aligned} \quad (1)$$

$$\begin{aligned} F &= \int E_L(t) \times E_L^*(t + \tau) \\ &= \int A_L(t) \times A_L^*(t + \tau) e^{-j\omega_0 t} \end{aligned} \quad (2)$$

where: the delay (τ) is set such that $\tau = T_{sym} - T_{CP}$; T_{sym} and T_{CP} are the symbol and cyclic prefix periods, respectively. The slow PDs define the integration period, averaging out the wide-band noise. Eqs. (1) and (2) also show that the phase change in E and F due to CFO averages out. After a fixed integration time, the signal is sampled once and a division operation (E/F) removes the common $e^{-j\omega_0 \tau}$ term. The $\int A_s(t) \cdot A_s^*(t + \tau)$ and

$\int A_L(t) \cdot A_L^*(t + \tau)$ terms end up being real-valued due to the cyclic prefix frame structure of the OFDM signal and as a result the frequency offset $\Delta\omega$ can be estimated (e.g. by a simple microprocessor) as:

$$\Delta\omega = \frac{-z(\frac{D}{E})}{\tau} \quad (\text{for } \tau=1\text{ns}, |\Delta f| \leq 500 \text{ MHz}) \quad (3)$$

Thus, there is no need for high-speed processing in the electronic domain. The theoretical estimation range can be calculated for $\tau=1\text{ns}$ to be ± 500 MHz and is verified in the simulations in next section.

Experimental setup and results

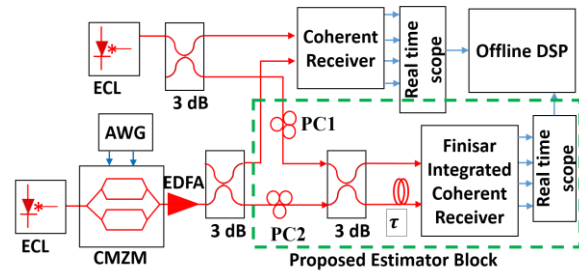


Fig. 2: Experimental setup; ECL: external cavity laser, CMZM: complex Mach-Zehnder modulator, AWG: arbitrary waveform generator

A practical implementation of Fig. 1 with fiber components would generate random phase differences between the inputs to the 90° hybrids, which would result in errors in the electro-optic estimator. Although this phase difference could be managed on an integrated photonic chip in the future, the setup requires modifications for our proof of concept experiment. For this, we exploit the polarization diversity receivers and use a single polarization signal (see Fig. 2).

The received and the LO signals are orthogonally polarized using polarization controllers (PC), combined and split using a 3-dB coupler where one of the output signals is delayed by τ and are fed to a polarization-diverse integrated coherent receiver (Finisar CPRV1b2tA) that contains two polarizing beam splitters (PBSs), two 90°-hybrids and balanced photodiodes connected as required in our design; except that here the PDs are high bandwidth. The input to the PBSs of the coherent receiver will then be $E_s(t) \hat{x} + E_L(t) \hat{y}$ and $E_s(t+\tau) \hat{x} + E_L(t+\tau) \hat{y}$, where $\hat{\cdot}$ denotes the polarization. The PBSs split the signals giving $(E_s(t), E_s(t+\tau))$ and $(E_L(t), E_L(t+\tau))$ at the inputs of the two 90°-hybrids as required in our actual design. By passing the signal and LO down the same physical fibers using polarization diversity, the phase drifts are equal on signal and LO and so are cancelled. The integration process provided by the slow PDs in Fig. 1 and low-rate processing was emulated in offline DSP in this proof of concept.

A 28-GBaud OFDM QPSK signal with 60 subcarriers and a 12% cyclic prefix was fed from arbitrary waveform generator (AWG) into an optical IQ modulator. These specifications lead to a delay, τ , of 1 ns. The modulated signal is split using a 3-dB coupler, where one output is connected to a coherent receiver and the other to the proposed FO estimator. The LO signal is also split in similar fashion. This splitting allows us to verify the accuracy of our proposed estimator by calculating the actual frequency offset using conventional offline DSP. This offline CFO estimation is achieved using the spectral peak search technique [1], using a 25-GHz bandwidth integrated coherent receiver connected to a 40-Gsa/s 30-GHz bandwidth real-time scope.

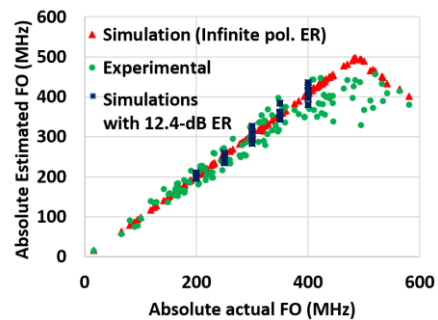


Fig. 3: DSP-estimated absolute FO vs. FO estimated by the proposed design.

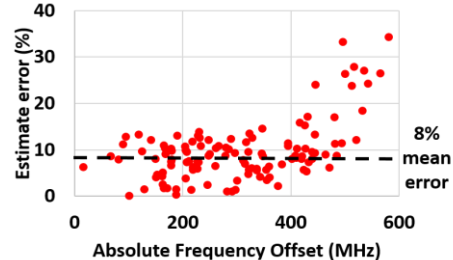


Fig. 4: Estimate error vs. freq. offset.

Fig. 3 shows the scatterplot of the estimation error of the proposed system, where the estimates have been compared with those calculated using the DSP technique. The simulations of the system, assuming ideal components, show excellent CFO tracking up to ± 500 MHz FO, followed by reversal of slope due to phase roll over in Eq. (3). This is close to where the measured CFO becomes uncertain (± 450 MHz). Fig. 4 shows the measured estimation error over a range of frequency offsets. The experimental results show a mean error of 8% over the range of ± 450 MHz FO with 3% standard deviation that causes the broadening of the scatterplot with increase in FO in Fig. 3.

In order to understand the reason for this estimation error, the system is simulated with different parameters to emulate uncertainties in experiment, such as the fluctuations in delay τ

due to temperature variations, random phase difference between two arms of the 3-dB coupler and the extinction ratio (ER) of the PBSs due to polarization misalignment. The fluctuations in τ and the phase difference between the arms of the 3-dB coupler were chosen randomly with a uniform distribution within the ranges $[-40, 40]$ ps and $[-\pi, \pi]$ respectively, and the polarization misalignment was varied from 0.5° to 10° , varying associated extinction ratio between 20.5 to 8 dB.

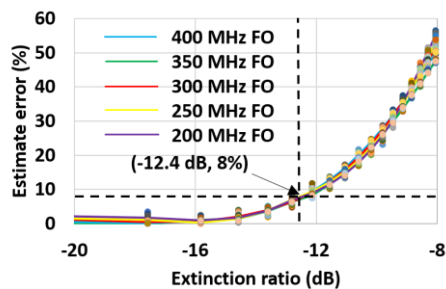


Fig. 5: Estimate error (%) vs. Extinction ratio (dB).

Fig. 5 shows that the effect of polarization misalignment θ ($ER=10\log_{10}(\sin[\theta])$) dominates as a source of systematic estimation error, while the random errors due to other parameters produce a relatively small scatter at different ER values. Also, the 8% systematic estimation error in Fig. 4 corresponds to $ER = 12.4$ dB or a 3.5° polarization misalignment. Setting this value in simulations, we observe a similar gradual increase in estimation error to that in Fig. 3 (blue dots), confirming that polarization misalignment is likely to be the dominant cause of error in experimental results over random errors due to other considered parameters.

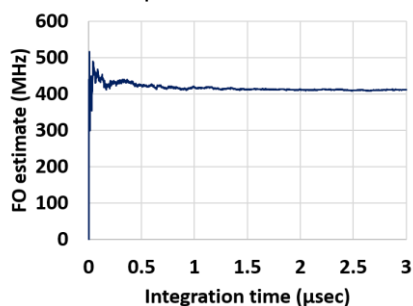


Fig 6: FO estimate vs. integration time of the slow PD.

Finally, to understand the sampling speed requirements of the system, Fig. 6 shows the convergence of the CFO estimate with integration time of slow photodiodes for a 410-MHz FO. The estimated value converges after $1.5 \mu\text{s}$. Thus, a single sample can be taken after $1.5 \mu\text{s}$, avoiding the need for a high-speed sampler.

The CFO estimation range of our device can be increased by reducing the delay τ , which additionally requires either an increase in baud rate, a reduction in number of subcarriers or an increase in the CP percentage.

Moreover, the error due to polarization misalignment could be avoided by implementing the proposed layout in Fig. 1 on a phase-stable photonic chip. This layout intrinsically allows for its use in polarization-multiplexed systems.

Although the autocorrelation averages out the AWGN noise and dispersion ISI cross terms, the robustness of the system under noise and chromatic dispersion remains to be investigated. As the concept of the system is based on time domain characteristics of the cyclic prefix, it can be extended for a single carrier system where pilot or training symbols are periodically transmitted, introducing cyclostationarity to the signal. Moreover, this cyclostationarity can be introduced regardless of modulation format and thus the concept can be generalized for any optical coherent communication system.

Conclusions

We have demonstrated a frequency offset estimator using electro-optic processing for optical OFDM systems, with the potential to be generalized for coherent optical communication systems. This system successfully estimated a CFO up to ± 500 MHz for 28-Gbaud QPSK modulated OFDM signal. The system does not need high-speed components, and provides a method for reducing the computational load on digital processors in coherent systems.

Acknowledgements

This work was made possible by Australian Research Council's Centre of Excellence (CUDOS - CE110001018) and Laureate Fellowship (FL130100041) schemes.

References

- [1] M.Selmi *et al.*, "Accurate digital frequency offset estimator for coherent PolMux QAM transmission systems," Proc. ECOC, P3.08, Vienna (2009).
- [2] Z. Liu *et al.*, "Homodyne OFDM with optical injection locking for carrier recovery," J. Lightwave Technol. Vol. 33, no. 1, p. 34 (2014).
- [3] Mingzhi Lu *et al.*, "A heterodyne optical phase-locked loop for multiple applications," Proc. OFC/NFOEC, OW3D.1, Anaheim (2013).
- [4] L. Naglic *et al.*, "Improved phase detector for electro-optical phase-locked loops," Electron. Lett. Vol. 44, no.12, p. 758 (2008).
- [5] Helmut Bölcskei, "Blind estimation of symbol timing and carrier frequency offset in wireless OFDM systems," IEEE Trans. J. Comm. Vol. 49, no. 6, p. 988 (2001).
- [6] Jingshi Li *et al.*, "A self-coherent receiver for detection of PolMux coherent signals," Opt. Express, Vol. 20, no. 19, p. 21413 (2012).
- [7] T. Fujita *et al.*, "Optical analog multiplier based on phase sensitive amplification," Proc. OECC, TuPS-8, Kyoto (2013).